Check for updates

Propellants, Explosives, Pyrotechnics

Propellants, Explosives, Pyrotechnics

RESEARCH ARTICLE OPEN ACCESS

Direct Measurement of Explosive Impulse From Contact to the Ultra-Near Field

R. Alford | R. Hazael | R. Critchley | L. Humphreys

Centre for Defence Engineering and Physical Science, Cranfield Defence and Security, Cranfield University, ShrivenhamSN6 8LA, Wiltshire, United Kingdom

Correspondence: R. Alford (roland.alford@cranfield.ac.uk)

Received: 18 September 2025 | **Revised:** 28 May 2026 | **Accepted:** 11 June 2026

Keywords: blast loading | contact detonation | explosive impulse | high-strain-rate effects | impulse–distance relationship | momentum transfer | near-field blast | ultra-near field

ABSTRACT

Measurement of impulse from explosive charges in contact and ultra-near-field regimes remains poorly characterised due to the short duration of loading, high strain rates, and the difficulty of obtaining direct momentum-based measurements. Existing approaches are predominantly pressure-derived or indirect, leading to uncertainty in the relationship between impulse, stand-off distance and explosive properties in regimes where detonation products directly interact with the target. This paper presents direct measurements of explosive impulse across contact and ultra-near-field conditions obtained using a ballistic pendulum system. The measurements span a range of explosive types, charge masses and stand-off distances, enabling systematic examination of impulse behaviour in regimes that are not well resolved in the open literature. The results demonstrate consistent and repeatable impulse measurements across the tested range and reveal clear relationships between impulse, stand-off distance and net explosive quantity. In particular, the data highlights the transition from contact-dominated loading to near-field behaviour and identifies asymptotic trends in impulse as stand-off increases within the geometric limits of the measurement system. Differences in behaviour between explosive types are also observed, indicating the influence of detonation characteristics on impulse delivery in the ultra-near field. The findings provide a directly measured dataset for explosive impulse in contact and ultra-near-field regimes and contribute to improved understanding of momentum transfer under these conditions. The implications for scaling, experimental design and interpretation of near-field explosive effects are discussed.

1 | Introduction

The ballistic pendulum was first invented by Benjamin Robins and was described in his groundbreaking work, *New Principles of Gunnery* in 1742 [1]. The general principle is that a pendulum follows the law of conservation of momentum, so the impact of a projectile travelling at some unknown velocity will transfer its energy into the pendulum, causing it to swing. The angle that the pendulum swings is directly related to the increase of momentum and from it, the velocity of the projectile can be determined. By measuring the maximum angle of rotation, if the length of the arm and mass of the bob is known, it is possible to derive the impulse [2].

Originally used as a means of calculating the velocity of projectiles, the ballistic pendulum is also widely used as a means of measuring the relative power of explosives [3, 4] and for measuring rocket thrust [5]. In more recent years small ballistic pendula have been used for testing one-shot digital micro thrusters that produce 10^{-4} Ns of impulse and are used to position nano satellites in orbit [6].

The SI unit for impulse is Ns, which is the force over time, which is equal to the change in momentum and is sometimes called the momentum impulse [7]. The simplest means of directly measuring the impulse is to use a ballistic pendulum.

This is an open access article under the terms of the Creative Commons Attribution License, which permits use, distribution and reproduction in any medium, provided the original work is properly cited.

© 2026 The Author(s). *Propellants, Explosives, Pyrotechnics* published by Wiley-VCH GmbH.

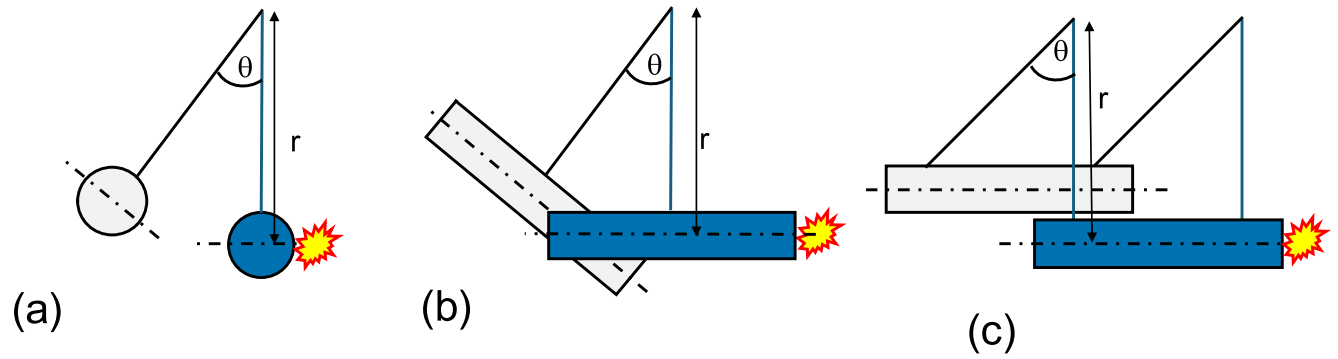

FIGURE 1 | Ballistic pendulum designs (not to scale) (a). Type 1—simple pendulum, (b) Type 1a, 1959 variant of Type 1 pendulum for measuring contact charges and (c) Type 2—horizontal pendulum with two suspension points.

Confusingly, the integral of the time-pressure history from pressure sensor data is frequently mis-described as the impulse. This may be due to the common use of pressure gauges for recording blast effects and the integration of the pressure-time histories which are then called impulse for simplicity. A dimensional analysis shows that this results in units of Pa.s or N.s/m^2 and is more properly the pressure impulse [8].

When considering the blast effects of explosions, the peak pressure gives little indication of the likely damage to structures, however the impulse, which indicates the momentum imparted, or the pressure-time history are both far more useful indicators; an extremely short duration of high pressure event may be completed before an object has time to react, whereas a lower pressure over a much longer period can have the potential to cause damage [9].

A literature review found several different designs for ballistic pendula [10–14], but the most common is a simple pendulum consisting of a simple ball, plate or bar suspended from a single fulcrum. A second design has a longitudinal mass suspended at two points along its length allowing a heavier mass to be used and to provide a degree of control of the swing.

For convenience, the different basic designs are referred to in this paper as Types 1, 2 and 3 and are shown in Figure 1.

Only one example of a system for measuring the impulse from direct contact charges has been found in literature from a Russian book on the physics of explosions published in 1959 [10]. The design is a variant of the Type 1 as it has a single fulcrum and is termed a Type 1a Pendulum in the paper. It featured a long bar of steel with a sacrificial impact plate attached to the charge end, suspended on what is possibly an adapted ballistic mortar frame.

Some Type 2 systems use Hopkinson Pressure Bars to record the pressure from the charges in addition to measuring the pendulum's swing [11].

Veldman et al. describe a Type 2 horizontal pendulum that is limited to non-contact charges in the near-field, ranging from 0.113 to 0.68 kg [14]. Critically, their method requires the use of a slow-motion camera and two exploding foil initiator detonators; one to initiate the test charge and a second to break a wooden dowel used to prevent the pendulum from pre-swinging. The last two requirements put their system beyond the reach of many researchers.

While most applications of the ballistic pendulum involve direct transfer of momentum into the system through the impact of projectiles or thrust from rockets attached to the pendulum, most explosive uses are restricted to non-contact measurements in which the force is applied by the shock wave from the explosive and the impact of combustion gases rather than the impact of a more conventional projectile. Charges are typically placed in the near field so that the pendulum is not damaged by the explosive effects of the test charges. This allows, for example, blast effects on structures to be investigated but does not allow the impulse from more powerful contact charges, such as those used in explosive demolition or explosive breaching to be measured.

1.1 | Momentum Impulse and Overpressure Impulse

When an explosive material detonates, it rapidly decomposes generating significant proportions of gas which expands outwards from the charge. In the case of an ideal spherical charge, the gases expand radially from the centre, preceded by a shock wave, formed by the compression of the air by the expanding gasses, travelling through the air [15]. In free air, when charges at close range detonate, the fireball extends up to and beyond the point of measurement, while at greater ranges the shockwave detaches from the fireball and continues for far greater distances. The initial shock wave velocity is higher during the initial stage before reaching a steady velocity close to the speed of sound [16]. At even greater ranges, the shock wave may lose energy and slow down below the speed of sound to form a sound wave that may still contain enough energy to cause damage in the same way that the blast from an explosion of a low-explosive such as black powder can cause damage despite not forming a shock wave [17].

Impulse is the change in momentum of a system and the impulse from explosive charges is a useful predictor of the damage or effect of charges resulting from the combination of the shockwave and overpressure and potentially fragment impact. Unfortunately, different methods of calculating the impulse leads to both inconsistency and confusion. A pendulum starts at rest and therefore has zero momentum. It swings to its maximum height at which its velocity is again zero (zero momentum) but

15214087, 0, Downloaded from https://onlinelibrary.wiley.com/doi/10.1002/prep.70242 by Mandy Smith - NICE, National Institute for Health and Care Excellence , Wiley Online Library on [13/07/2026]. See the Terms and Conditions (https://onlinelibrary.wiley.com/terms-and-conditions) on Wiley Online Library for rules of use; OA articles are governed by the applicable Creative Commons License

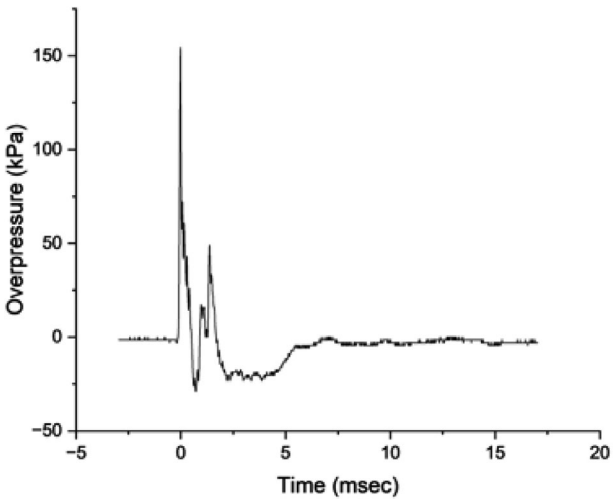

FIGURE 2 | Typical Friedlander waveform time-history curve shows multiple peaks from complex reflections (EX-392) which complicate any measurement of impulse based on the pressure history which are based on the area under the curve. This results in the impulse per unit of area (kPa.s or N.s/m^2) rather than classical impulse, which has a unit of N.s.

on its return to the starting position, it has maximum velocity and maximum momentum. As we know that the initial momentum is zero, the maximum momentum is therefore equal to the impulse.

The SI unit of Impulse is N.s. The unit for momentum is normally kg.m/s, but is dimensionally equivalent to N.s. This is sometimes referred to as the momentum impulse. Other terms used are the incident impulse (I_i) and reflected impulse (I_r) [18]. The incident impulse is distinct from the reflected impulse, but both the incident and reflected impulses are types of momentum impulse.

The most significant source of confusion about impulse is that it is widely stated that impulse is the integral of a Friedlander Pressure–Time history of an explosion, specifically at non-near-field distances [19]. This would allow a pressure sensor to be used to measure the impulse from an explosion without requiring any other equipment, such as a ballistic pendulum. Unfortunately, a unit analysis shows that this is not the case. The units from a pressure-time history are Pa.s or N.s/m^2 which is the impulse per unit area. While this is a useful thing to know for a specific point in space, it gives no indication of the effect such a blast would have on a body of more complex shape and assumes that the blast is even across the body, which is often not the case. This is sometimes referred to as the *pressure impulse* despite not strictly being an impulse.

The *overpressure impulse* (I_{op}) is the integrated area under the pressure-time curve of an explosion (Kingery C. N. and Bulmash G, 1984), and is therefore a function of the pressure, duration of the blast wave and the rate of decay of the pressure behind the shock wave (Figure 2). This is broadly the same as the *pressure impulse* described earlier, but the incident overpressure is specifically the pressure above ambient caused by a blast wave as it propagates through air before it interacts with any surface whereas the pressure impulse is a more general and less specific term. Importantly, in blast physics, this impulse does not directly represent momentum change but rather the energy content delivered by the blast wave over time. Given the relative simplicity of determining this when measuring blasts using pressure gauges, this is the form of impulse commonly used in blast physics [20]. When using such pressure sensors, care must be taken to ensure that the correct orientation of the gauge is used to measure either the incident pressure (pressure travelling across the surface of the sensor) or the reflected pressure (in which the pressure is normal to the surface of the sensor). The sampling frequency and pressure range of the gauges must also be matched to the expected blast overpressure.

For the avoidance of confusion, unless otherwise stated, impulse is used to mean momentum impulse throughout this paper.

1.2 | Measuring Impulse From Contact and Near-Field Charges

Contact charges, and those in the very near-field, apply pressures an order of magnitude higher than those from non-charges in free air due to the shockwave interaction giving rise to brisant-phase propulsion. The target material in contact with a detonating charge experiences the brisant effect of the charge; an effect that is measured in the dent test which measures the size and depth of the dent formed in a steel target and which can be used to estimate the Chapman–Jouguet (CJ) pressures [21].

If a contact charge is considered, even the tiniest of charges will inevitably destroy any pressure sensor rendering them useless for this sort of measurement. As a result, little research appears to have been conducted into measuring impulse from charges in direct contact or extremely near field. This is partly because most research interests lie in such fields as building and vehicle protection, but also because it is technically harder to do, given the violent nature of explosives and the propensity to damage equipment [11, 22, 23].

Despite this, there are real-world applications in which contact charges are used, for example, in commercial demolition and military breaching, for which the present research is relevant. A simple method of measuring the impulse from contact and near-field charges would be very useful for these applications, and the ballistic pendulum would be the obvious tool for this if they could be made to survive the damage caused by the shock from repeated detonations of contact charges.

Most designs lack a means of preventing catastrophic damage to the equipment and are therefore not suitable for use with direct contact explosive charges or even those with a stand-off, but are in close proximity to the contact surface. This may best be defined in terms of scaled distance, which is the distance divided by the cube root of the explosive charge weight with a scaled distance of approximately 0.2 sometimes used in literature as a practical definition of near-field [14].

They also tend to have limited ranges of charge size dictated by the structural strength of the system, the mass of the pendulum bob, length of pendulum arm and the accuracy of measurement of the rotation. In essence, a system robust enough to withstand the massive forces of explosive contact charges will typically be too massive to record movements from small charges. Small

15214087, 0, Downloaded from https://onlinelibrary.wiley.com/doi/10.1002/prep.70242 by Mandy Smith - NICE, National Institute for Health and Care Excellence , Wiley Online Library on [13/07/2026]. See the Terms and Conditions (https://onlinelibrary.wiley.com/terms-and-conditions) on Wiley Online Library for rules of use; OA articles are governed by the applicable Creative Commons License

systems might have a range of 0.75–100 g of explosive [12] while large systems may be used with charges of 1–10 kg of explosive at distances of 500–1000 mm [13, 24]. The lack of a convenient and practical system has meant that most real-world applications have typically been designed empirically without a clear understanding of the impulse required or produced by such charges. Such charges include kicking charges for use in commercial demolition and military breaching charges for knocking down doors and blowing holes in walls. The prohibitive cost of building realistic targets or the inability to experiment on representative conditions have meant that most charges are designed with a high degree of trial and error and experience rather than any scientific analysis resulting in finite element analysis being more commonly used in place of physical testing [25].

Charges at greater stand-off distances do not produce the extremely high-brisance shocks of contact charges and the impulse is therefore imparted by the incident shockwave and impact from the explosive gases and at even greater distances, the shockwave alone. At these ranges, the surface area and shape of the pendulum become increasingly influential in the measured response.

1.3 | Scope

The purpose of this paper is to describe the design, implementation, and experimental evaluation of a ballistic pendulum for measuring explosive impulse in contact and ultra-near-field configurations. The focus is on establishing the measurement capability, repeatability, and practical applicability of the technique. Interpretation of impulse coupling mechanisms, stand-off-dependent behaviour or underlying physical regimes lies outside the scope of this paper and are addressed separately.

2 | Materials and Methods

2.1 | Design of Pendulum/Modular Ballistic Pendulum (MBP) Design

2.1.1 | Modular Ballistic Pendulum

The MBP described in this paper has a rugged steel frame and a series of interchangeable horizontally supported bobs, ranging from 86 to 750 kg, sacrificial and semi-sacrificial impact plates, suspension chains to give a pendulum arm length of approximately 1.3 m and a simple but accurate method of recording the swing requiring only a standard 4k video camera. This allows the system to be used with bare contact charges as well as charges suspended in the near-field with a minimum amount of recording equipment, typically by a single person.

Tests were conducted with bare charges of various types of explosive, both in contact and with a stand-off. Charges ranged from 1.25 g up to almost 700 g resulting in swings as small as 0.5° and as great as 45°, although it was subsequently recognised that for some of the assumptions to hold true, the maximum angle is 14°. The errors when measuring very small swings are clearly proportionally greater than when measuring swings in the 5°–15° range. It was observed that very large swings led to twisting of the suspension frame resulting in artificially high impulses being recorded.

The MBP consists of a rigid steel frame approximately 2 m × 3 m × 1 m and a series of pendulum bobs suspended on chains (Figure 3).

The standard construction of the bob is a length of I-beam at least 1 m in length with 30 mm steel plates welded to each end, one acting as the impact face for the charges and the other as a counterbalance. Additional, semi-sacrificial steel plates are bolted to the welded plates to provide additional stiffness and mass.

The chains were attached to two lugs welded to the top flange of the I-beam and two parallel pairs of lugs on the frame that position the bob horizontally and allow longitudinal swings while limiting lateral yaw movements. The chains were rated to at least three times the mass of the heaviest bob. The lifting lugs are 30″ (762 mm) apart which were used as a design parameter for the location of the pivots.

The pivot would ideally, be a knife-edge, however the requirement to be able to swap the bobs quickly and easily led to the selection of off-the-shelf lifting chains with pre-fixed shackles. These were fitted to rings fitted to the frame and to the lugs on the bobs. It was found that the orientation of the rings on the frame was critical to ensure that the most frictionless orientation was selected.

For contact charges, rectangular steel plates 250 mm × 400 mm × 30 mm are bolted onto the bob's fixed impact face in place of the steel disc. When being used to measure free-air stand-off charges, the rectangular impact face plates are replaced by a circular steel disc 500 mm in diameter and 40 mm thick which is bolted to the bob's fixed impact face.

Small charges are measured using the light and medium bobs when a single additional plate is used giving a total thickness of 60 mm, including the impact face welded to the bob. For larger charges, the heavy mass is used two plates are used giving a total thickness of 90 mm to ensure that the impact face is not deformed. The bolted-on plates are considered semi-sacrificial.

The heavy mass was constructed using a BLU-109 bomb case with a steel plate welded to the base, allowing additional, semi-sacrificial plates to be bolted on. The original suspension lugs are used and their spacing, 30″ (762 mm) apart, was the reason the standard spacing between suspension lugs for all the masses was fixed at this distance.

Charges fired in the same position on the plates eventually began to erode the surface. This effect could be slowed down by minor adjustments to the charge location (left or right) of a few millimetres. The charges were not large enough to bend or deform the plates which were strongly supported by the main, welded base plates. After approximately 100 firings, the plate was simply reversed to present a flat surface and ultimately, was replaced with a new plate after the surface became rough and pitted. As the plate was not bent, it continued to present a flat surface for the

15214087, 0, Downloaded from https://onlinelibrary.wiley.com/doi/10.1002/prep.70242 by Mandy Smith - NICE, National Institute for Health and Care Excellence , Wiley Online Library on [13/07/2026]. See the Terms and Conditions (https://onlinelibrary.wiley.com/terms-and-conditions) on Wiley Online Library for rules of use; OA articles are governed by the applicable Creative Commons License

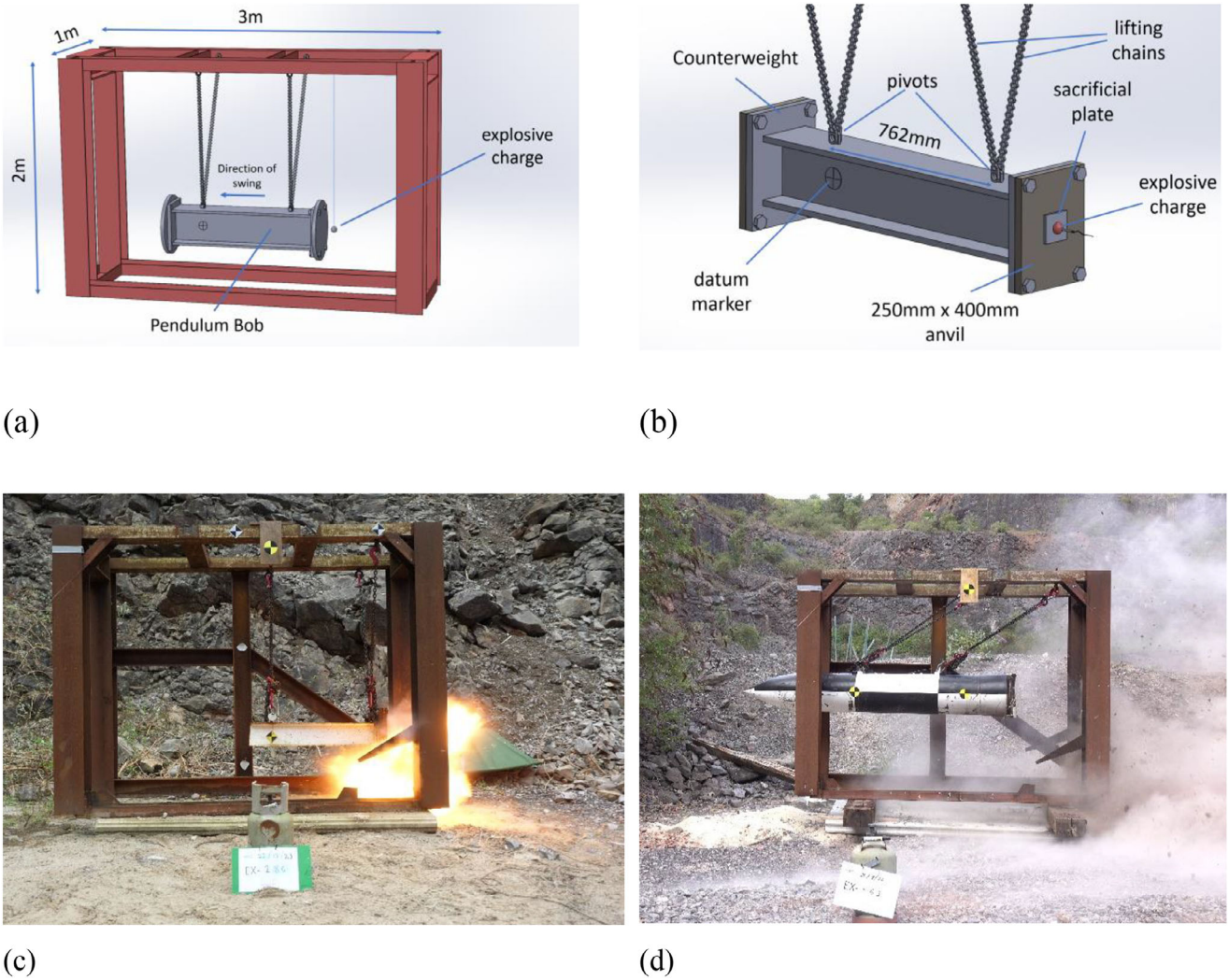

FIGURE 3 | (a) Illustration of MBP frame and mass. (b) The smaller pendulum masses are fabricated from I-beam sections and the explosive charges may be fixed directly to the impact face. (c) I-section 86 kg mass in use. (d) The 763 kg mass is a repurposed BLU-109 bomb case can measure up to 2000 Ns.

charges to be fixed to, ensuring good contact, which is considered important so as not to skew results. The data did not, however, show any variation in results as the plates became progressively pitted.

For high-brisance explosives such as military plastic explosives, additional sacrificial plates 100 mm × 100 mm × 10 mm are fixed to the larger plates using adhesive tape [26]. The number of smaller plates depends on the type and size of contact charges with either two or three plates used. Their mass was added to the pendulum mass for calculations.

2.1.2 | Calculating Impulse Using a Horizontal Pendulum

Impulse is defined as the change in momentum of a system. A ballistic pendulum can be used to calculate the impulse using the angle of rotation and the known constants of the pendulum. The impulse is the entire impulse from a charge into the system and takes no account of the area of the pendulum [27].

As the horizontal pendulum is turned through 90° from the vertical pendulum used by Battelle, the equation used for calculating the impulse is changed to:

$$J = m\sqrt{2gr(1-\cos\theta)} \quad (1)$$

where: J = impulse (Ns), m is mass of pendulum (kg), g = gravity (m/s^2), r = distance of centroid of the pendulum to the rotational axis (m), and θ = angle of rotation (degrees).

There are a few derivations of equations for calculating impulse for a ballistic pendulum in literature [12, 28–30]. Battelle has one of the more complete derivations but is for a vertical pendulum (the mass is projected vertically). All the derivations are based on conservation of momentum and derive the horizontal or vertical component of the momentum depending on which plane the impulse is acting. The following derivation is adapted from Battelle but resolves to a slightly simpler final form for a horizontal rather than vertical pendulum.

Impulse from the charge will cause the pendulum centre of mass (COM) to have an initial velocity (v) causing the pendulum

15214087, 0, Downloaded from https://onlinelibrary.wiley.com/doi/10.1002/prep.70242 by Mandy Smith - NICE, National Institute for Health and Care Excellence , Wiley Online Library on [13/07/2026]. See the Terms and Conditions (https://onlinelibrary.wiley.com/terms-and-conditions) on Wiley Online Library for rules of use; OA articles are governed by the applicable Creative Commons License

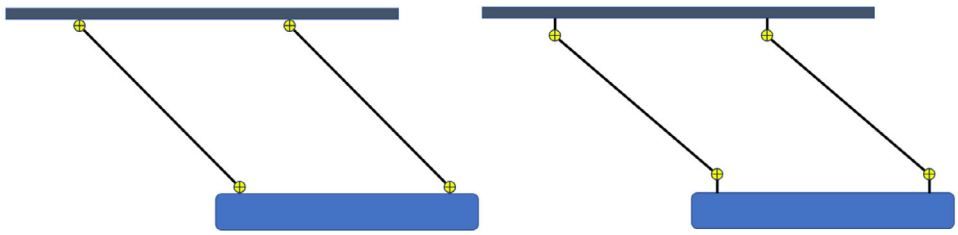

(a) (b)

FIGURE 4 | (a) Mode 1 swing and (b) Mode 2 swing.

to have an initial angular velocity (w). Gravity acts against the motion of the pendulum and the final angle of rotation can be used to determine the work done. Figure 1c shows the geometries used for the derivation.

For the rotation of a rigid body around a fixed point, the energy–work equation is:

$$\underset{\text{(work)}}{\frac{1}{2}I\omega^2_{\text{(initial)}}} + \underset{\text{(PE)}}{mgh_{\text{(initial)}}} = \frac{1}{2}I\omega^2_{\text{(final)}} + mgh_{\text{(final)}} \tag{2}$$

where, I is moment of inertia (kg m^2), w is angular velocity, m is mass of pendulum (kg), g is gravity and h is height raised (m). Under the initial conditions, h is zero. Under the final conditions, when the pendulum has stopped, w is zero. So, the energy–work equation becomes:

$$\frac{1}{2}\mathrm{I}\ \omega^2_{\text{(initial)}} = mgh_{\text{(final)}} \tag{3}$$

Since, $\omega = v/r$ and $h = r(1 - \cos\theta_{\text{(final)}})$where, v = velocity (m/s) and θ is the final angle of the pendulum, the equation becomes:

$$\frac{1}{2}I\frac{v^2}{r^2}_{\text{(initial)}} = mgr(1 - \cos\theta_{\text{(final)}}) \tag{4}$$

Since, $I = mr^2$

$$\frac{1}{2}mv^2{}_{\text{(initial)}} = mgr(1 - \cos\theta_{\text{(final)}}) \tag{5}$$

That is, KE = PE

$$\frac{1}{2}\ v^2 = gr\,(1 - \cos\theta) \tag{6}$$

solving for v:

$$v = \sqrt{2gr\,(1 - \cos\theta)} \tag{7}$$

Conservation of momentum dictates that the initial angular momentum divided by the length of the arm will be equal to the momentum of the pendulum centre of gravity from the impulse of the charge:

$$J = I\omega/r_{\text{(pendulum)}} = Iv/r^2_{\text{(pendulum)}} = mv_{\text{(final)}} - mv_{\text{(initial)}} \tag{8}$$

where, J is impulse (Ns) and is the change in momentum, $mv_{\text{(final)}}$—$mv_{\text{(initial)}}$. Since $mv_{\text{(initial)}}$ is equal to zero the Impulse (J) from the charge so:

$$J = mv_{\text{(final)}} \tag{9}$$

Therefore,

$$J = m\sqrt{2gr(1 - \cos\theta)} \tag{10}$$

2.1.3 | Pendulum Length

The length of the pendulum arm is measured from the pivot at the top to the COM. With a simple pendulum, it is common to treat the effect of the mass of the suspension chains or cables as insignificant [31] but with the lighter mass, this assumption cannot be made. The MBP design uses bobs with significant mass which require suitably robust suspension chains that add significantly to the overall mass. The total mass of the bob must include the mass of the chains, and this can result in the COM moving towards the pivot in the Y-axis. With the lighter bob, the mass of the chains is a significant proportion of the total mass (bob: 55 kg, chains: 31 kg).

Simply measuring the distance from the pivot to the centre of the bob is inaccurate. An alternative method of determining the pendulum length, based on the period of swing was found to be a simple method that allows the effective length to be determined for each firing. As shown in Figure 4, there are two main possible modes of swinging, either with the chain and fixings all acting as a single unit (Mode 1) or where the secondary fixing point forms a pivot (Mode 2), which has the effect of shortening the pendulum length. Mode 2 tends to occur when the light pendulum mass is used with heavy charge weights.

The equation of motion for a simple pendulum is a second-order linear differential equation which is not trivial to solve, however, the *small angle approximation* may be applied [31, 32]. This states that when the angle is small and measured in radians, the sine of the angle is approximately equal to the angle itself. This may be expressed as:

$$\sin\theta \approx\ \theta \tag{11}$$

This holds true for angles less than approximately 0.24 radians (14°) for which the error remains below 1% [33]. Applying this simplifies the equation which may then be rearranged to solve

15214087, 0, Downloaded from https://onlinelibrary.wiley.com/doi/10.1002/prep.70242 by Mandy Smith - NICE, National Institute for Health and Care Excellence , Wiley Online Library on [13/07/2026]. See the Terms and Conditions (https://onlinelibrary.wiley.com/terms-and-conditions) on Wiley Online Library for rules of use; OA articles are governed by the applicable Creative Commons License

(a) (b) (c)

FIGURE 5 | Image resolution is important for the accurate capturing of data from video. (a) Full frame (3840 × 2160 pixels) video image. (b) The same image zoomed in on bob. Distance between black and yellow squares is 1 m. (c) Image zoomed in further showing the vertical line displaying a 1-pixel resolution.

for the period T.

$$T = 2\pi\sqrt{\frac{L}{g}} \tag{12}$$

where T is the period of oscillation, L is the pendulum arm length and g is acceleration due to gravity. Note that this is a simplified equation that is valid for small swings (below approximately 14° [34]. Rearranged to solve for L this equation becomes:

$$L = \frac{T^2 g}{4\pi^2} \tag{13}$$

This allows the COM to be calculated by determining the period of the pendulum, which can be done easily from video recordings of the motion. This is important because the horizontal bob design with a fixing point/pivot on the top edge of the bob means that a simple datum marker on the bob is not necessarily on the axis of the pendulum. If the angle of rotation is greater than 14° the *small angle approximation* cannot be used, and so smaller calibration charges may be used to determine the pendulum length which can then be used for calculations for larger charges that give greater swings.

The period-derived equivalent length implicitly captures the physical pendulum's inertia distribution via $L_{eq} = I/(mr_{COM})$; impulse is then obtained via angular impulse about the pivot using the effective moment arm to the loading point.

2.2 | Data Capture and Processing

The first ballistic pendulum in 1742 used a loosely gripped length of ribbon to measure the travel of the pendulum [1]. Since then, numerous methods of capturing data from ballistic pendula have been used successfully [1, 2, 11, 12, 28]. The standard method for capturing data from a ballistic pendulum is to measure the angle of rotation of the pendulum arm [35]. As technology has advanced, various methods have been utilised, including built-in protractors, rotary transition transducers, laser displacement gauges and Hopkinson Bars [11, 22, 28].

A method that would allow simple, rapid and accurate data capture by a single operator also conducting the explosive tests was desired, so all these methods were discounted. The method uses video footage to capture the rotation and computer software to analyse and measure the movement [12]. This does not need special hardware to capture and process electrical signals and is less prone to damage or failure. Video data capture was therefore selected for this design. A video analysis program called *Tracker*, developed as part of Open-Source Physics was used to measure the angle of rotation and the lateral movement [36].

Standard digital cameras recording video at Ultra HD resolution (3840 × 2160 pixels) recorded at a frame rate of 29.97 fps to capture results. Two models of camera were used; a Sony RX-10 with a 24–200 mm F2.8 lens was used in early tests and was subsequently upgraded to a Lumix GH5 with a 12–60 mm F3.5-5.6 lens which has significantly better poor-light capabilities [37]. The better optics of the Lumix meant that when zoomed in to detail on videos, the image was far clearer despite both cameras claiming to be 4k cameras. There is no requirement for faster frame rates as the swing is slow enough to easily capture the apogee at normal frame rates. Figure 5a shows the raw resolution obtained from video footage. Filming at UHD or 4K resolution allowed the tripod-mounted camera to be positioned approximately 1 m above the ground and 10 m away. This was far enough from the MBP to use the camera with a neutral focal length to reduce parallax effects on the image. The image resolution is great enough to allow the image to be zoomed in on to allow easy measurement of the movement of the bob using the Tracker software.

The fireball from a typical test with 5 g of explosive, producing 14.5 Ns of impulse lasts only one frame (33 ms) of standard-speed video recording while the pendulum takes about 16 frames, just over half a second, to reach the apogee. This affords ample time to measure the motion of the pendulum.

The *tracker* software used for video analysis allows images to be zoomed in and out to allow calibration of images as well as automatic tracking and data capture from videos (Figure 6). The ultimate limitation on the amount of zoom that can be used is the

15214087, 0, Downloaded from https://onlinelibrary.wiley.com/doi/10.1002/prep.70242 by Mandy Smith - NICE, National Institute for Health and Care Excellence , Wiley Online Library on [13/07/2026]. See the Terms and Conditions (https://onlinelibrary.wiley.com/terms-and-conditions) on Wiley Online Library for rules of use; OA articles are governed by the applicable Creative Commons License

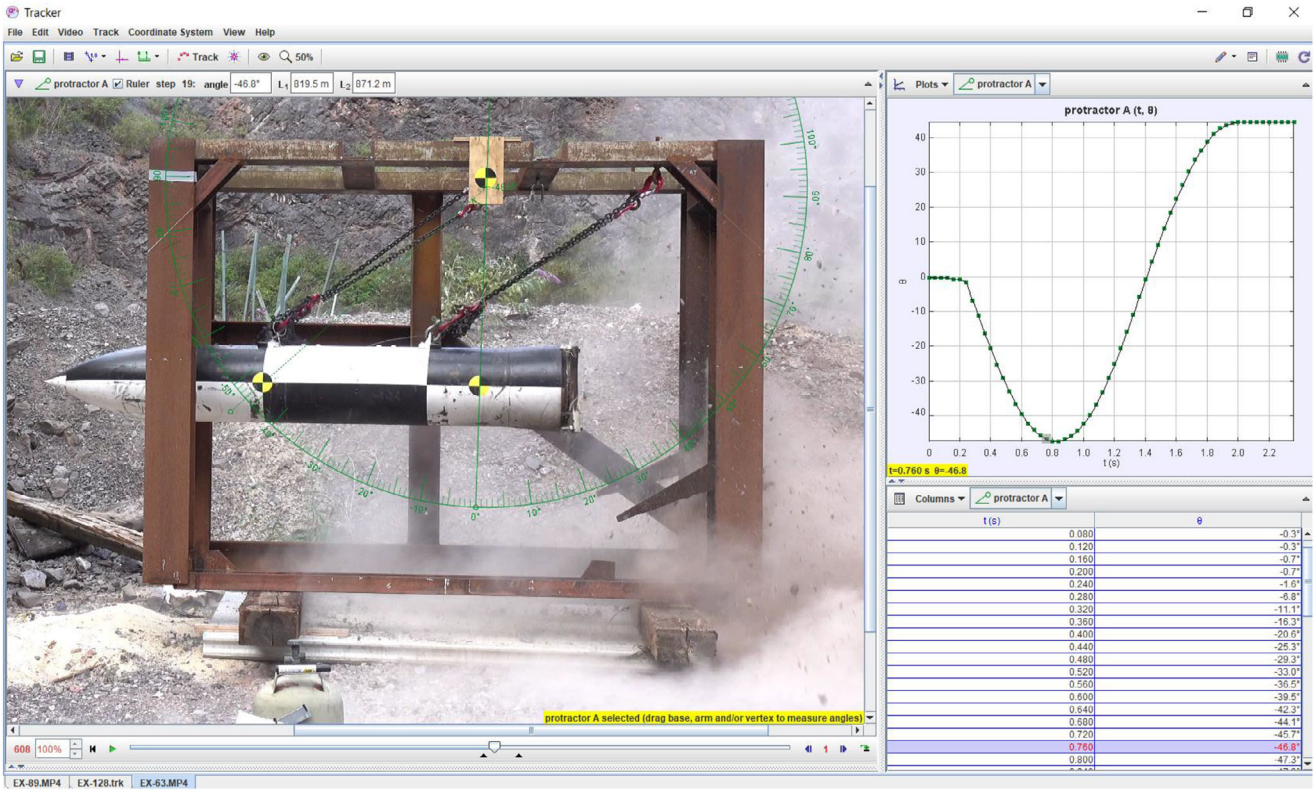

FIGURE 6 | Tracker allows automatic or manual point tracking which allows the movement of the pendulum to be plotted.

TABLE 1 | Sources of error.

	Source of error	Description
1	Pre-swing—bob	Bob not static at moment of firing
2	Mechanical losses and friction	Pivot and connections between chain and shackles
3	Twisting of frame	MBP frame twisting when heavy bob is used with large charges
4	Unbalanced bob	Bob constructed without counterbalance
5	Pre-swing—charge	Explosive charge swinging
6	User-variation	Consistency of reading video data
7	Non-axial loading	Contact charges not symmetrically positioned
8	Camera parallax	Camera not aligned on the axis of the chain being measured

point at which features being measured are approximately 1 pixel wide (see Figure 5c.)

2.3 | Errors

The main errors identified are listed in Table 1 below:

The top four sources of error are discussed here, while a more complete assessment of uncertainty sources and error propagation is provided in Supporting Information B.

Residual pendulum motion at the moment of firing violates the assumption of zero initial momentum and can introduce a positive or negative bias depending on swing phase as shown in Table 2. This effect was mitigated by ensuring the pendulum was stationary prior to firing; tests exhibiting observable pre-swing were excluded from analysis.

Mechanical losses and friction were minimised through careful configuration of the pivot and are considered negligible relative to the measured impulse.

At high impulses with the heaviest bob, frame torsion was observed, defining an upper operational limit for the current configuration; data exceeding this limit were excluded.

Early tests with an unbalanced bob showed sensitivity to pitch under higher impulses; subsequent tests used counterbalanced bobs, eliminating this effect.

15214087, 0, Downloaded from https://onlinelibrary.wiley.com/doi/10.1002/prep.70242 by Mandy Smith - NICE, National Institute for Health and Care Excellence , Wiley Online Library on [13/07/2026]. See the Terms and Conditions (https://onlinelibrary.wiley.com/terms-and-conditions) on Wiley Online Library for rules of use; OA articles are governed by the applicable Creative Commons License

TABLE 2 | Pre-swing sensitivity.

Bob (kg)	Explosive	NEQ (g)	Angle (°)	Impulse (N.s)	Deviation (°)	Momentum (N.s)	Error (± %)
86	Detcord	1.25	0.8	3.8	0.1	0.5	13.2
86	Detcord	20	8.9	42.5	0.1	0.5	1.2
237	PE4	20	2.3	30.7	0.1	1.3	4.2
237	PE4	60	6.5	86.7	0.1	1.3	1.5
758	Poladyn	100	1.8	78.2	0.1	4.3	5.5
758	Poladyn	500	11	477.1	0.1	4.3	0.9

(a) (b)

FIGURE 7 | Charge configuration and fixing was changed as appropriate for each series: (a) contact charges attached to sacrificial impact and (b) spherical charges suspended on a thread.

2.4 | Explosives Tested

Three different types of explosives, plastic explosive (PE4), dynamite (Poladyn) and emulsion (Emulex 2+) were weighed and hand-rolled into approximate spheres and formed into hemispherical contact charges by pressing them onto sacrificial steel plates mounted on the pendulum impact face (Figure 7a). The inherent adhesion of the explosives was sufficient to maintain placement during preparation.

Sacrificial plates were manufactured from mild steel and measured 100 mm × 100 mm × 10 mm. Depending on explosive type, one or more plates were used and attached directly to the pendulum bob.

A limited number of detonating cord tests were conducted during method development; these are mentioned for completeness but are not central to the validation results presented.

Contact charges were affixed directly to the impact face. For stand-off and non-contact configurations, charges were formed into spheres and suspended on a fine thread from the frame above the pendulum, with stand-off adjusted using a magnet. Unless otherwise stated, stand-off was measured from the centre of the charge to the impact face. One test series reproduced prior work by Veldman, in which stand-off was measured from the nearest point of the charge to the impact face.

All charges were initiated using standard commercial No. 8 electric detonators [38]; unlike the arrangement used by Veldman et al. [14], the present configuration does not require synchronised dual initiation or exploding foil initiators.

2.5 | Repeatability and Uncertainty

Repeatability of the ballistic pendulum measurements was assessed through multiple nominally identical shots conducted under the same experimental conditions. Representative repeated firings showed low shot-to-shot variation relative to the changes observed between different charge sizes and configurations. For example, two repeated PE4 firings at 50 g NEQ and 200 mm stand-off produced impulses of 20.5 and 21.5 N.s, respectively, corresponding to a coefficient of variation of approximately 3.2%.

15214087, 0, Downloaded from https://onlinelibrary.wiley.com/doi/10.1002/prep.70242 by Mandy Smith - NICE, National Institute for Health and Care Excellence , Wiley Online Library on [13/07/2026]. See the Terms and Conditions (https://onlinelibrary.wiley.com/terms-and-conditions) on Wiley Online Library for rules of use; OA articles are governed by the applicable Creative Commons License

This demonstrates that the pendulum response is sufficiently repeatable to resolve meaningful differences in impulse within the experimental programme. Additional repeatability data are provided in Supporting Information A.

3 | Test Plan

3.1 | Variables

The objective of the experiments was to test the MBP with different configurations and to validate the design. The main variables were as follows:

- Contact/Non-contact charges
- Pendulum bob mass
- Type of explosive—plastic explosive, detonating cord, dynamite, packaged emulsion
- Stand-off distance for non-contact charges.

3.2 | Summary of Test Series

The experiments were broken down into five series, each designed to test the MBP in particular ways based on the variables described above. The experiments presented in this paper can be broadly split into two categories: contact charges and non-contact charges. The first series explores the effect of changing the pendulum bobs was done using contact charges as this reduces any potential factors arising from the surface area of the impact face and gas wraparound effects.

Series 2 and 3 compared different explosives, with contact and non-contact charges to rank them by impulsiveness.

Series 4 examined the effect of stand-off distance using two explosives, PE4 and Emulex 2+.

Series 5 repeated the experiments done by Veldman [14] in which C4 charges of various NEQs were fired 127 mm from the pendulum. The full test series are summarised in Table 3 below:

4 | Results and Discussion

Note that a full set of results is given in Supporting Information A. A detailed interpretation of how explosive properties influence loading duration and variability is beyond the scope of this paper and is addressed separately.

4.1 | Series 1: Effect of Changing the Pendulum Mass

Series 1 examined whether measured impulse depends on pendulum bob mass.

The three pendulum bobs, light, medium and heavy, weighed 128.8, 328.4 and 758.4 kg, respectively. Poladyn was used, with charge masses ranging from 10 to 673 g, selected to suit each bob with partial overlap between datasets.

The results for each pendulum bob are shown in Figure 8. All linear regressions were constrained to pass through the origin, consistent with zero impulse at zero NEQ. Allowing an unconstrained intercept did not materially change the fitted gradients or the conclusions drawn.

Impulse increased linearly with NEQ for all three pendulum bobs.

Linear regression of impulse against NEQ yielded gradients of 0.845, 0.842 and 0.927 N.s g^{-1} for the light, medium and heavy bobs, respectively. The light and medium bobs gave near-identical gradients, while the heavy bob produced a slightly higher gradient. Figure 8d shows all three datasets plotted together, demonstrating consistent, colinear behaviour across pendulum masses

In an ideal measurement system, the impulse–NEQ gradient would be independent of pendulum mass. The present results indicate broadly consistent behaviour Across pendulum masses, although a small systematic mass- or charge-range-dependent effect cannot be excluded. The most likely contributors are proportionally lower mechanical losses at higher impulses, differences in charge size/diameter affecting Poladyn performance, or improved coupling at larger charge masses. The data therefore support use of the MBP across masses, while indicating that

TABLE 3 | Summary of test series investigating how consistently the Pendulum records the impulse from similar charges when different pendulum masses are used.

Ser.	Range	Test	Explosive	No. firings
1	Contact	Effect of changing pendulum mass	Poladyn	18
2	Contact	Investigating the effect of changing the explosive	PE4, Poladyn, Emulex 2+	19
3	Non-contact	Investigating the effect of changing the explosive	PE4, Poladyn, Emulex 2+	16
4	Non-contact	Characterising the effect of changing the stand-off	PE4, Emulex 2+	40
5	Non-contact	Fixed SO, varying NEQ (repeat of Veldman tests)	C4	5

15214087, 0, Downloaded from https://onlinelibrary.wiley.com/doi/10.1002/prep.70242 by Mandy Smith - NICE, National Institute for Health and Care Excellence , Wiley Online Library on [13/07/2026]. See the Terms and Conditions (https://onlinelibrary.wiley.com/terms-and-conditions) on Wiley Online Library for rules of use; OA articles are governed by the applicable Creative Commons License

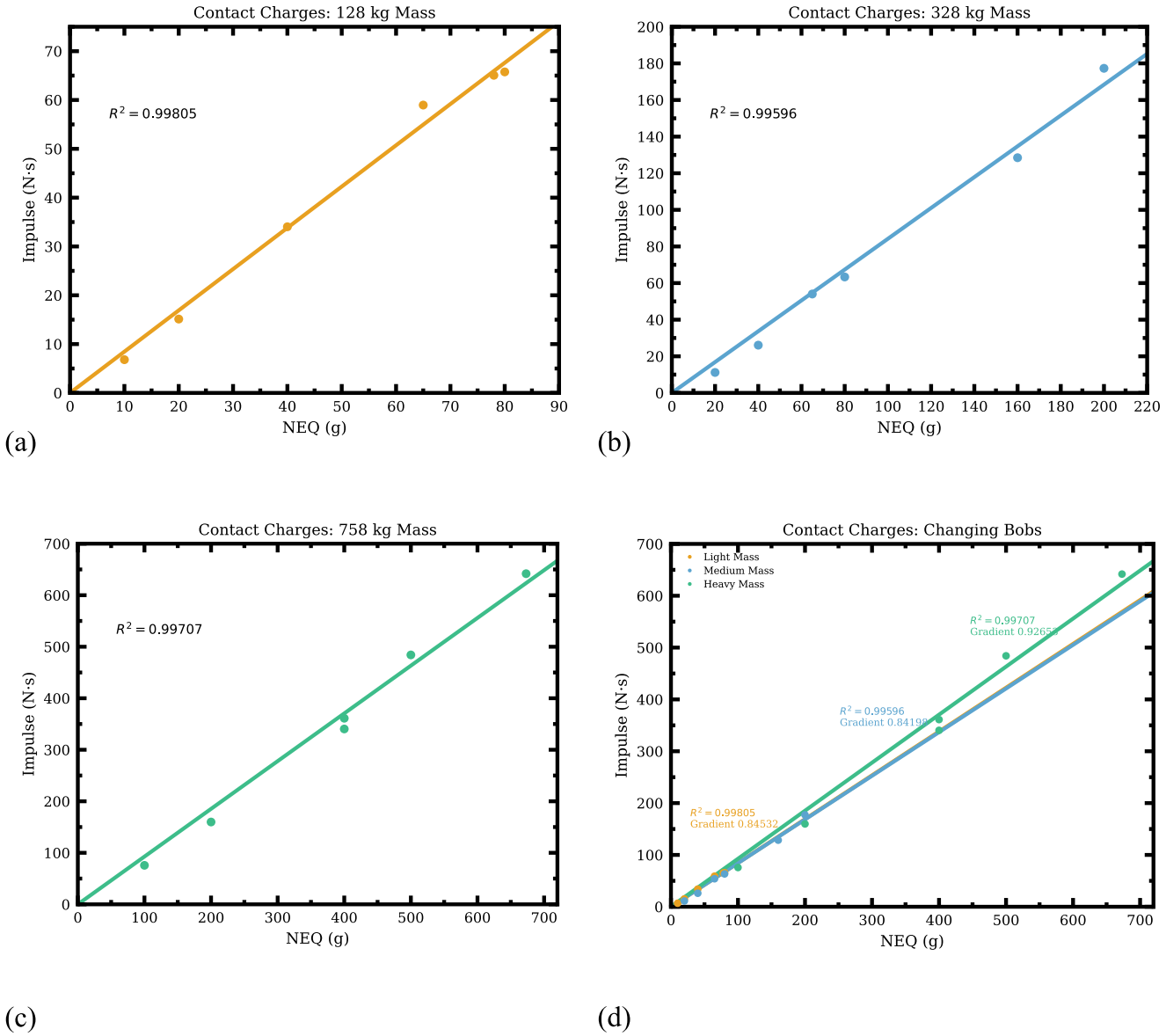

FIGURE 8 | (a–c) The data sets for each of the pendulum bobs with Poladyn and (d) combined data.

pendulum mass and charge range should not be treated as entirely interchangeable without calibration

The marginally higher gradients observed for the heaviest bob may reflect mechanical losses that are approximately constant rather than proportional to bob mass; however, this effect cannot be isolated within the present dataset. All results presented in this paper are therefore based on the period-derived pendulum length.

4.2 | Series 2: Changing Explosives With Contact Charges

Figure 9 compares the impulse–NEQ relationships for PE4, Poladyn and Emulex 2+ under contact conditions. PE4 produced the highest impulse per unit NEQ under contact conditions, followed by Poladyn and Emulex 2+. Poladyn produced approximately 57% and Emulex 2+ approximately 42% of the impulse generated by PE4. Compared with PE4 and Poladyn, Emulex 2+ exhibits

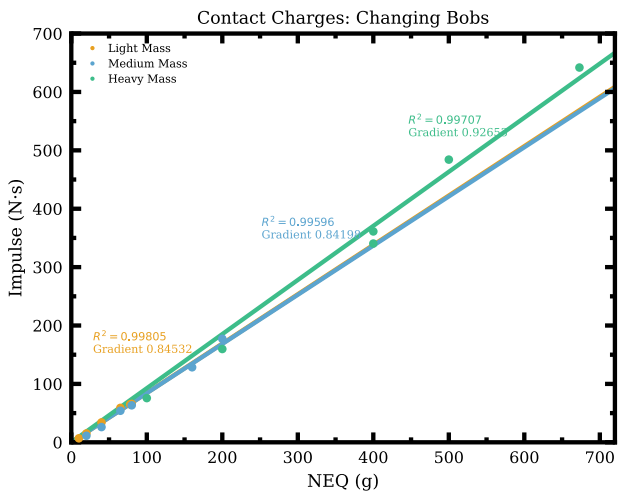

FIGURE 9 | The NEQ-impulse characteristics for PE4, Poladyn and Emulex 2+.

15214087, 0, Downloaded from https://onlinelibrary.wiley.com/doi/10.1002/prep.70242 by Mandy Smith - NICE, National Institute for Health and Care Excellence , Wiley Online Library on [13/07/2026]. See the Terms and Conditions (https://onlinelibrary.wiley.com/terms-and-conditions) on Wiley Online Library for rules of use; OA articles are governed by the applicable Creative Commons License

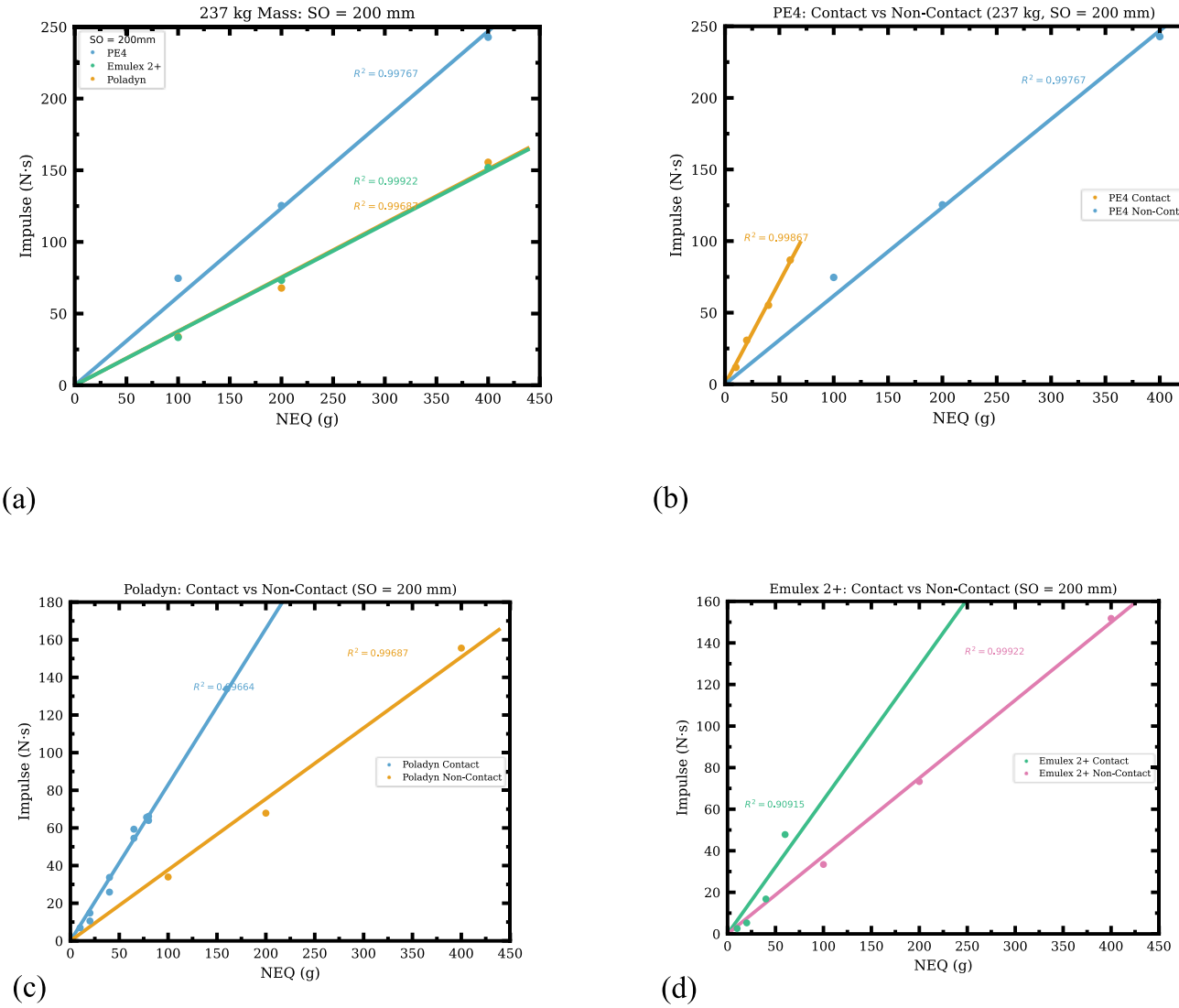

FIGURE 10 | (a) PE4, Poladyn and Emulex 2+ at 200 mm SO and (b–d) comparison of contact and non-contact charges.

greater scatter about the fitted trend, reflected in a lower r^2 value.

The observed ranking broadly follows expected detonation performance trends, with the higher-VoD explosive (PE4) producing the greatest impulse under contact conditions. This is consistent with the stronger brisant loading associated with higher detonation velocity explosives. However, impulse transfer is not governed by detonation velocity alone, and factors including explosive density, heat of explosion, gas expansion behaviour and charge geometry are also likely to influence the measured response.

The present results, therefore, likely reflect the combined influence of brisant shock loading, gas expansion behaviour, explosive density, heat of explosion, reaction zone characteristics, charge geometry and loading duration. The greater scatter observed in Emulex 2+ may reflect increased sensitivity to variations in coupling associated with lower-VoD, longer-duration loading behaviour.

4.3 | Series 3: Changing Explosives With Non-Contact Charges

Having established that the MBP design can be used for contact charges, it was then used with non-contact charges suspended away from the impact face. No sacrificial plates were required as the airgap between the charge and the pendulum removed the brisant effect that is the main cause of damage.

The next series repeated the investigation of Series 2 with charges suspended 200 mm from the pendulum rather than in contact. The same three explosives, PE4, Poladyn, Emulex 2+ were used and explosive quantities varied from 50 up to 400 g.

The results are given in Figure 10. As the NEQ increased, the impulse increased in a linear manner, but what was notable is that unlike contact charges, the results for Poladyn and Emulex 2+ at a stand-off were almost colinear. Poladyn produced 37.2% less impulse and Emulex 2+ 36.9% less than PE4.

15214087, 0, Downloaded from https://onlinelibrary.wiley.com/doi/10.1002/prep.70242 by Mandy Smith - NICE, National Institute for Health and Care Excellence , Wiley Online Library on [13/07/2026]. See the Terms and Conditions (https://onlinelibrary.wiley.com/terms-and-conditions) on Wiley Online Library for rules of use; OA articles are governed by the applicable Creative Commons License

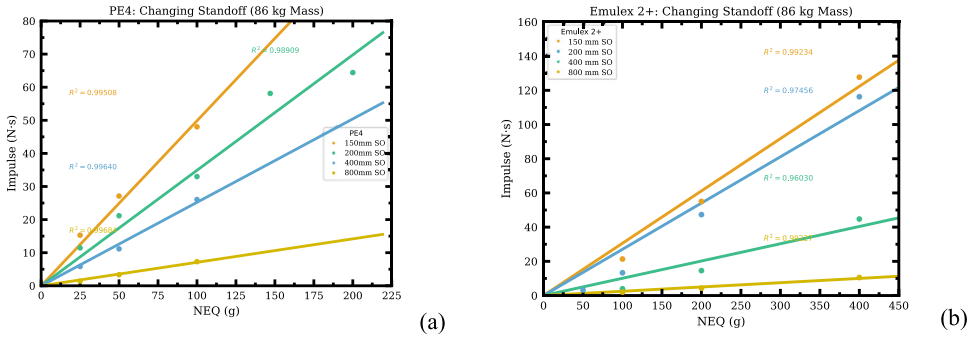

FIGURE 11 | (a) PE4 data show good linearity at all distances, and (b) data for Emulex 2+ shows similar linearity.

For non-contact charges at 200 mm stand-off, Poladyn and Emulex 2+ exhibited near-colinear impulse–NEQ behaviour, despite differing manufacturer-reported properties (Figure 10). What is notable from the specifications is that both Poladyn and Emulex 2+ have very similar heats of explosion. When compared with PE4, they are both approximately 21% lower than PE4, whereas the experimental stand-off impulse gradients were approximately 37% lower than PE4, indicating that just as it is in the VOD of an explosive [39], the heat of explosion could be an important factor in the impulse produced, but it is not a simple linear relationship.

A notable feature of the 200 mm stand-off data is that Poladyn and Emulex 2+ exhibit almost identical impulse-NEQ gradients despite producing substantially different gradients under contact conditions. This suggests that the strong dependence on brisant loading observed in rigid contact configurations evolves at stand-off distances where momentum transfer increasingly reflects the combined effects of blast-wave propagation and gas expansion. The results, therefore, indicate that explosive ranking based on contact impulse does not directly translate to stand-off configurations, and that the relative behaviour of explosives may change significantly as stand-off increases.

The increased scatter observed for Emulex 2+ may reflect differences in the temporal characteristics of loading associated with lower detonation velocity explosives. If the effective loading duration is longer, small variations in coupling may lead to increased variability in measured impulse. The same effect may also contribute to the lower contact impulse measured for Emulex 2+ relative to the more brisant explosives tested, particularly in rigid contact configurations where short-duration brisant loading may dominate momentum transfer. However, the overall impulse–NEQ relationship remains linear, and the assumption of impulsive loading is considered valid within the resolution of the present measurements.

In addition, differences in bulk density change the physical size of a given NEQ charge; for centre-referenced stand-off measurements this alters the surface-to-target distance between explosives at the same NEQ, which may contribute to apparent differences and scatter at stand-off. Poladyn has a higher bulk density (≈1.6 g/cm^3) than Emulex 2+ (≈1.2 g/cm^3), such that for a given NEQ the Emulex charges have a larger physical radius; for centre-referenced stand-off measurements this increases the effective surface-to-target distance and may contribute to differences and increased scatter observed at stand-off. While density influences charge size and detonation pressure, the time-history of product expansion is governed by the detonation process and product EOS; detailed treatment is beyond the scope of this paper.

4.4 | Series 4: Investigating the Effect of Varying Stand-Off of Non-Contact Charges

PE4 was tested using the light bob and Emulex 2+ tested with the medium pendulum bob with a 500 mm diameter steel disc fitted. Sets of firings with various NEQs were conducted at 150, 200, 250, 400 and 800 mm stand-off, measured from the centre of the charge. The NEQ was varied from 25 to 400 g. The results are given in Figure 11.

For Emulex 2+, an unconstrained linear fit indicates a consistent non-zero intercept (equivalently, an apparent NEQ offset) across series; the origin-constrained fit remains linear but yields a lower r^2. The origin offset may reflect systematic differences in coupling and/or measurement sensitivity at low impulses; detailed interpretation is beyond the scope of this paper.

Replotting the same data with NEQ against stand-off distance reveals a strongly non-linear attenuation behaviour, characterised by a rapid initial reduction in impulse out to approximately 400 mm followed by more gradual decay at larger stand-offs (Figure 12). The stand-off dependence is well represented by a power-law relationship of the form $I = a.\mathrm{SO}^b$, consistent with the non-linear attenuation expected in ultra-near-field blast loading. The fitted exponents were broadly similar across the charge masses tested, indicating comparable attenuation behaviour over the stand-off range examined.

Compared with PE4 at equivalent NEQs, Emulex 2+ exhibited consistently steeper attenuation exponents, indicating a more rapid reduction in measured impulse with increasing stand-off distance. This is consistent with the broader observation that the relative behaviour of the explosives changes between contact and stand-off configurations, suggesting differing contributions from brisant loading and gas expansion processes.

The differing attenuation behaviour produces an apparent crossover region in which Emulex 2+ generates greater measured impulse than PE4 at very small stand-off distances, while PE4 produces greater impulse at larger stand-offs. This further illustrates that explosive ranking is strongly dependent on loading geometry and stand-off configuration. However, because the

15214087, 0, Downloaded from https://onlinelibrary.wiley.com/doi/10.1002/prep.70242 by Mandy Smith - NICE, National Institute for Health and Care Excellence , Wiley Online Library on [13/07/2026]. See the Terms and Conditions (https://onlinelibrary.wiley.com/terms-and-conditions) on Wiley Online Library for rules of use; OA articles are governed by the applicable Creative Commons License

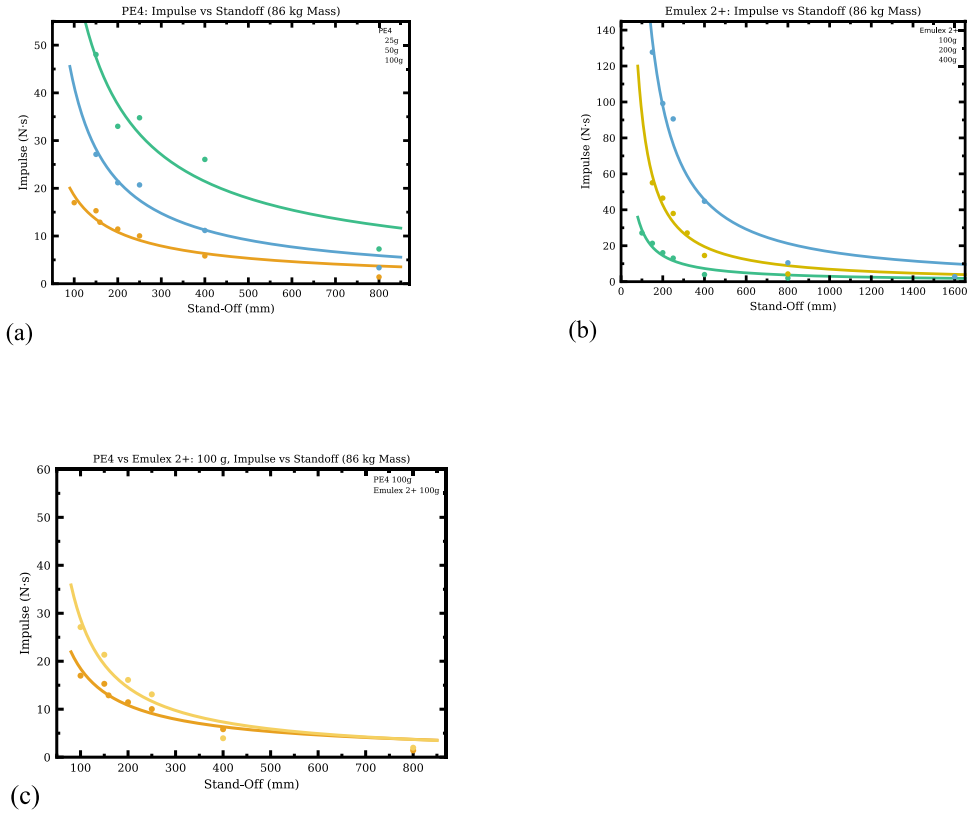

FIGURE 12 | (a) The same data from Figure 11a (PE4) replotted with NEQ v Impulse show an asymptotic regression, (b) Emulex 2+ data shows a similar regression and (c) PE4 and Emulex 2+ data for 100 g charges are plotted against each other to show the difference in relative performance of the two explosives.

fitted exponents are derived from a limited number of stand-off positions, both the exponent values and the precise crossover location should be interpreted cautiously and treated primarily as descriptive rather than mechanistic parameters.

4.5 | Series 5: Comparison With Veldman et al

Tests replicating the stand-off definition used by Veldman et al. were conducted to confirm compatibility of measurement conventions (Figure 13). Veldman et al. used a circular steel strike face of 0.574 m diameter, corresponding to an exposed area of approximately 0.259 m^2. The MBP impact disc used in the present comparison was 0.500 m diameter, corresponding to approximately 0.196 m^2. Veldman's exposed strike area was therefore approximately 32% larger than that used here. This represents a potential geometric difference between the systems, although the contribution of the outer annulus is expected to be reduced because blast loading decreases with radial distance from the charge axis.

This difference in impact-face diameter represents an upper bound on geometric effects; because loading decays with radial distance, the effective contribution of the outer annulus is expected to be smaller.

The comparison with Veldman et al. shows good overall agreement despite substantial differences in pendulum geometry, pendulum mass, target face dimensions, and experimental

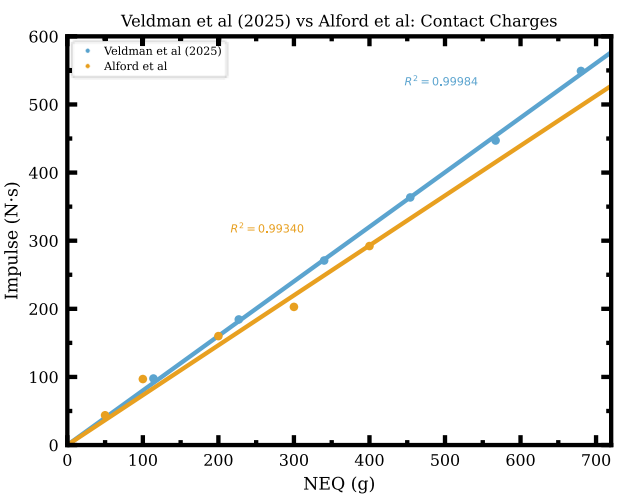

FIGURE 13 | Veldman's tests were repeated using the MBP and compared. (Alford et al. (this paper)).

configuration. The gradient obtained in the present work (0.732 N.s g^{-1}) is moderately lower than that reported by Veldman et al. (0.801 N.s g^{-1}), but remains within the same overall range and follows the same linear impulse–NEQ behaviour. This is consistent with the broader observation that pendulum mass and apparatus configuration may introduce modest systematic differences in measured gradients, while still supporting the general validity and reproducibility of the ballistic pendulum approach across different experimental systems.

15214087, 0, Downloaded from https://onlinelibrary.wiley.com/doi/10.1002/prep.70242 by Mandy Smith - NICE, National Institute for Health and Care Excellence , Wiley Online Library on [13/07/2026]. See the Terms and Conditions (https://onlinelibrary.wiley.com/terms-and-conditions) on Wiley Online Library for rules of use; OA articles are governed by the applicable Creative Commons License

5 | Conclusions

This research has demonstrated that the ballistic pendulum, in its modular form, remains a practical and effective method for measuring momentum impulse from both contact and near-field explosive charges. The MBP developed in this study proved capable of surviving repeated detonations, accommodating a wide range of explosive types and net explosive quantities, and delivering consistent and reproducible results. Taken together, the statistical comparison of gradients supports the use of multiple pendulum bobs with broadly consistent behaviour across masses, although small systematic differences between configurations cannot be fully excluded.

The principal findings can be summarised as follows:

- *Validation of the MBP design*—Consistency across pendulum masses confirms that mechanical losses and geometric effects are well controlled, enabling confidence in the conservation-of-momentum approach.
- *Contact vs. non-contact behaviour*—Contact and non-contact charges produce measurably distinct impulse responses. The MBP reliably resolves differences in impulse behaviour across charge type and stand-off.
- *Stand-off dependence*—The impulse–distance relationship exhibits an asymptotic trend over the stand-off range tested, illustrating the response characteristics of the MBP.
- *Comparison with published data*—Results align with existing studies while avoiding the complexity and fragility of high-speed sensors or multi-detonator systems.

The MBP therefore provides a robust, low-cost and versatile tool for experimental blast research, particularly where pressure gauges cannot survive contact or near-field conditions. Beyond validating empirical design practices, it offers a scalable platform for quantifying impulse in demolition, breaching and protective structure applications.

Future work will investigate the physical mechanisms governing stand-off-dependent impulse coupling and regime transition.

Acknowledgements

This work was supported by Alford Technologies Ltd, which provided logistical and technical resources. The sponsor had no role in study design, data collection, analysis, interpretation, article preparation or the decision to submit for publication.

Ethics Statement

The authors confirm that this article is original, has not been published previously, and is not under consideration elsewhere. The work presented reflects the authors' own research and analysis and is reported accurately and in full. All contributors who meet authorship criteria are appropriately credited, and all authors have made substantial contributions to the work and approve the submitted version. Relevant prior work is properly acknowledged, and all sources are cited in accordance with academic standards. The authors confirm compliance with the publication's ethical policies and accept responsibility for the integrity of the work.

Conflicts of Interest

Roland Alford has a relationship with Alford Technologies Ltd, including board membership, employment, equity ownership, non-financial support and travel reimbursement. He is also the majority shareholder, Chairman and CTO of the Alford Group. Roland Alford is named on patents held by Alford IP Ltd.

Data Availability Statement

The data that support the findings of this study are available in the Supporting Information of this article.

Use of Generative AI and AI-Assisted Technologies in the Writing Process

Large language models were used as structured dialogue tools during the development of this work. Specifically, ChatGPT (OpenAI), Google Gemini (Google DeepMind), Grok (xAI) and Perplexity Ai were used to assist in organising author-generated notes, developing article structure and section framing, and refining phrasing, supporting data visualisation workflows, and assisting with the generation and refinement of publication-quality graphs and figures. All outputs were treated as provisional and were not incorporated without critical assessment and substantive modification by the authors. The authors conducted iterative review and refinement to ensure technical accuracy and coherence. The conception of the work, interpretation of results, synthesis of arguments, all technical positions and final technical conclusions, and all literature identification and referencing remain the authors' exclusive original intellectual contribution. AI tools were occasionally used to suggest potential literature directions; however, all sources were independently identified, retrieved and verified using conventional academic databases, and no AI-generated references have been included. These tools were not used for citation generation or as sources of factual authority. All technical content has been independently verified by the authors, who assume full responsibility for the accuracy, originality and integrity of the work.

References

1. B. Robins, *New Principles of Gunnery* (The Richmond Publishing Co Ltd, 1972). Reprint of 1742 edition.

2. J. M. Milutinović, N. P. Hristov, D. D. Jerković, S. Z. Marković, and A. B. Živković, "The Application of the Ballistic Pendulum for the Bullets Velocity Measurements," In IOP Conference Series: Materials Science and Engineering. (IOP Publishing, 2019). 012016, https://doi.org/10.1088/1757-899X/659/1/012016.

3. L. C. Taylor, R. R. Skaggs, and W. Gault, "Vertical Impulse Measurements of Mines Buried in Saturated Sand," *Fragblast* 9, no. 1 (2005 Mar): 19–28, https://doi.org/10.1080/13855140500125557.

4. The War Office. Text Book of Explosives Used in The Service, (His Majesty's Stationary Office, 1938).

5. Sandia Lab News. Rocket Pendulum Used in Shock Testing Here. (Sandia Lab News, 1955 Jun 3).

6. D. L. Lewis, S. W. Janson, R. B. Cohen, and E. K. Antonsson, "Digital Micropropulsion," *Sensors and Actuators A: Physical* 80, no. 2 (2000): 143–154, https://doi.org/10.1016/S0924-4247(99)00260-5.

7. T. Gelbord, "Momentech—Modern Explorations of the Impulse-Momentum Theorem," *Rosenheim Technical University of Applied Sciences* (2024): 18–25.

8. A. Ghadirian and H. Bredmose, "Pressure Impulse Theory for a Slamming Wave on a Vertical Circular Cylinder," *Journal of Fluid Mechanics* 867 (2019 May 25): R1, https://doi.org/10.1017/jfm.2019.151.

9. P. Smith. "Blast Effects on Buildings," In *Blast Effects on Buildings*. (Emerald Publishing Limited, 2009 Jan), https://doi.org/10.1680/BEOB2E.35218.

15214087, 0, Downloaded from https://onlinelibrary.wiley.com/doi/10.1002/prep.70242 by Mandy Smith - NICE, National Institute for Health and Care Excellence , Wiley Online Library on [13/07/2026]. See the Terms and Conditions (https://onlinelibrary.wiley.com/terms-and-conditions) on Wiley Online Library for rules of use; OA articles are governed by the applicable Creative Commons License

10. F. A. Baum, K. P. Staniukovich, and B. I. Shekhter, "Physics of an Explosion (Chapter XI)," In: Physics of an Explosion. (1959), 507–518. (T-1488 (a-q)).

11. T. J. Cloete and G. N. Nurick, "Blast Characterization Using a Ballistic Pendulum With a Centrally Mounted Hopkinson Bar," *International Journal of Protective Structures* 7, no. 3 (2016): 367–388, https://doi.org/10.1177/2041419616663535.

12. M. Fjällgren, D. Wood, G. J. Appleby-Thomas, and S. Mohammed, "Investigation on Fundamental Physics Underpinning Water Based Disruptors" [Master's Thesis]. (Cranfield Defence and Security, Cranfield University, 2019 Jul.).

13. A. Iluk, "Modeling and Evaluation of Loads in Vehicles Subjected to Mine Blast," *Solid State Phenomena* 220–221 (2015): 207–212, https://doi.org/10.4028/www.scientific.net/SSP.220-221.207.

14. R. L. Veldman, M. W. Nansteel, R. Yang, and C. C.-T. Chen, "Ballistic Pendulum Measurement and Prediction of Blast Reflected Impulse From Spherical Charges at Close Standoff Distances," *Propellants, Explosives, Pyrotechnics* 50, no. 1 (2025 Jan): e202400106, https://doi.org/10.1002/prep.202400106.

15. C. H. Johansson and P. A. Persson, *Detonics of High Explosives* (London and New York: Academic Press, 1970).

16. J. M. Gordon, K. C. Gross, and G. P. Perram, "Fireball and Shock Wave Dynamics in the Detonation of Aluminized Novel Munitions," *Combust Explos Shock Waves* 49, no. 4: (2013 Jul): 450–462, https://doi.org/10.1134/S0010508213040084.

17. I. von Maltitz, *Black Powder Manufacturing, Testing & Optimizing. Dingman's Ferry* (American Fireworks News, 2003).

18. C. N. Kingery and G. Bulmash. Airblast Parameters From TNT Spherical air Burst and Hemispherical Surface Blast. Aberdeen Proving Ground, MD 21005: US Army Ballistic Research Laboratory, (ARDC, 1984 Apr), Report ARBRL-TR-02555.

19. V. Karlos, G. Solomos, and M. Larcher. Analysis of Blast Parameters in the Near-Field for Spherical Free-air Explosions [JRC Technical Reports]. Joint Research Centre, (European Union /European Commission JRC, 2016), 74. JRC Technical Reports nos: JRC101039, EUR 27823. https://doi.org/10.2788/778898.

20. C. E. Needham, D. Ritzel, G. T. Rule, S. Wiri, and L. Young, "Blast Testing Issues and TBI: Experimental Models That Lead to Wrong Conclusions," *Frontiers in Neurology* 6 (2015 Apr 8): 1–10, https://doi.org/10.3389/fneur.2015.00072.

21. G. Pimbley, A. Bowman, W. Fox, J. Kershner, C. Mader, and M. Urizar, "Investigating Explosive and Material Properties by use of the Plate Dent Test [Internet]. Los Alamos, New Mexico: Los Alamos Scientific Laboratory (LASL)," (1980 Nov), [cited 2025 Apr 11]. Report LA-8591-MS, https://www.osti.gov/servlets/purl/6742166/doi:10.2172/6742166.

22. S. E. Rigby, A. Tyas, R. J. Curry, and G. S. Langdon, "Experimental Measurement of Specific Impulse Distribution and Transient Deformation of Plates Subjected to Near-Field Explosive Blasts," *Experimental Mechanics* 59, no. 2 (2019 Feb 15): 163–178, https://doi.org/10.1007/s11340-018-00438-3.

23. E. G. Pickering, S. C. K. Yuen, and G. N. Nurick, "The Influence of the Height of Burial of Buried Charges—Some Experimental Observations," *International Journal of Impact Engineering* 58 (2013): 76–83, https://doi.org/10.1016/J.IJIMPENG.2013.03.001.

24. S. D. Clarke, S. D. Fay, J. A. Warren, A. Tyas, S. E. Rigby, and I. Elgy, "A Large Scale Experimental Approach to the Measurement of Spatially and Temporally Localised Loading From the Detonation of Shallow-buried Explosives," *Measurement Science and Technology* 26, no. 1 (2015 Jan 1): 015001, https://doi.org/10.1088/0957-0233/26/1/015001.

25. A. A. Khalil, "Enhanced Modeling of Steel Structures for Progressive Collapse Analysis Using the Applied Element Method," *Journal of Performance of Constructed Facilities* 26, no. 6 (2012 Dec): 766–779, https://doi.org/10.1061/(ASCE)CF.1943-5509.0000267.

26. Breacher's Tape LLC. Breacher's Tape [Internet]. 2022 [cited 2022 Aug 29], https://www.breacherstape.com/product-p/bt30.htm.

27. J. Shin, A. S. Whittaker, and D. Cormie, "Incident and Normally Reflected Overpressure and Impulse for Detonations of Spherical High Explosives in Free Air," *Journal of Structural Engineering* 141, no. 12 (2015 Dec): 04015057, 10.1061/(ASCE)ST.1943-541X.0001305.

28. Battelle Memorial Institute. Characterization of EOD Explosives Access Tools [Final Report]. 505 King Avenue, Columbus, OH: Battelle Memorial Institute; 2002 Mar. (Technical Support Working Group (TSWG); T-1301).

29. A. Arnold, "An Analysis of Impulse From Tamped Explosives" [Master's Thesis]. Shrivenham, UK: Cranfield Defence and Security, Cranfield University; 2021 Jul.

30. Ballistic Pendulum/Projectile Launcher Instruction Manual [Internet]. PASCO Scientific; 2011 Sep [cited 2022 Mar 8]. Report nos: 012-05375C, pasco.com.

31. D. A. Russell. "Acoustics and Vibrations Animations [Internet]." (The Pennsylvania State University, 2018). Oscillation of a Simple Pendulum, https://www.acs.psu.edu/drussell/Demos/Pendulum/Pendulum.html.

32. D. G. Tolasa, "Theoretical Analysis of a Simple Pendulum Experiment," *International Journal of Current Research in Science, Engineering & Technology* 8, no. 1 (2025 Apr 21): 214–218, 10.30967/IJCRSET/Diriba-Gonfa-Tolasa/168.

33. J. J. Bissell, "Proof of the Small Angle Approximation Sin $\theta \approx \theta$ Using the Geometry and Motion of a Simple Pendulum," *International Journal of Mathematical Education in Science and Technology* 56, no. 3 (2025 Mar 4): 548–554, https://doi.org/10.1080/0020739X.2023.2258885.

34. J. E. Drotleff, C. T. Vincent, S. A. Mullin, J. D. Walker, and B. L. Morris. Research in Close-in Blast Loading From High Explosives [Contractor Report]. FMC Corporation, Santa Clara; 1996 Sep. Contractor Report ARL-CR-308.

35. HyperPhysics [Internet]. Georgia State University; [cited 2022 Dec 1]. Ballistic Pendulum, http://hyperphysics.phy-astr.gsu.edu/hbase/Class/PhSciLab/balpen.html.

36. D. Brown, W. Christian, and R. M. Hanson. Tracker Video Analysis and Modelling Tool [Internet]. [cited 2022 Aug 29], https://physlets.org/tracker/.

37. Panasonic. Lumix GH5 (DC-GH5 Body Only) [Internet]. [cited 2024 Feb 17], https://www.panasonic.com/uk/consumer/cameras-camcorders/lumix-mirrorless-cameras/lumix-g-cameras/dc-gh5body.html.

38. Société Davey Bickford. Daveydet Electric Detonator [Technical Data Sheet]. 2008.

39. K. G. Balachandar and A. Thangamani, "Design of New Energetic Materials Based on Derivatives of 1,3,5-trinitrobenzenes: A Theoretical and Computational Prediction of Detonation Properties, Blast Impulse and Combustion Parameters," *Heliyon* 6, no. 1 (2020 Jan): e03163, https://doi.org/10.1016/j.heliyon.2020.e03163.

Supporting Information

Additional supporting information can be found online in the Supporting Information section.

Supplementary File 1: prep70242-sup-0001-SuppMat.pdf

Supplementary File 2: prep70242-sup-0002-SuppMat.docx

15214087, 0, Downloaded from https://onlinelibrary.wiley.com/doi/10.1002/prep.70242 by Mandy Smith - NICE, National Institute for Health and Care Excellence , Wiley Online Library on [13/07/2026]. See the Terms and Conditions (https://onlinelibrary.wiley.com/terms-and-conditions) on Wiley Online Library for rules of use; OA articles are governed by the applicable Creative Commons License

https://dspace.org/

Direct measurement of explosive impulse from contact to the ultranear field

Alford, Roland; Hazael, Rachael; Critchley, Richard; Humphreys, Lisa

2026-12-31
Wiley
https://doi.org/10.1002/prep.70242
Alford R, Hazael R, Critchley R, Humphreys L. (2026) Direct measurement of explosive impulse from contact to the ultranear field. Propellants, Explosives, Pyrotechnics, Available online 12 July 2026, Article number e70242

Downloaded from a DSpace repository. https://dspace.org/